

Direct Bit Loading With Reduced Complexity and Overhead for Precoded OFDM Systems

Fatma Kalbat, *Member, IEEE*,
 Arafat Al-Dweik , *Senior Member, IEEE*,
 Youssef Iraqi , *Senior Member, IEEE*,
 Husam Mukhtar , *Member, IEEE*,
 Bayan Sharif , *Senior Member, IEEE*,
 and George K. Karagiannidis , *Fellow, IEEE*

Abstract—This paper considers the bit loading problem for communication systems that utilize orthogonal frequency division multiplexing (OFDM) in conjunction with precoding (POFDM) or time-domain interleaving (IOFDM). In particular, we propose a new bit loading algorithm for P/I-OFDM that has substantially higher effective throughput and less computational complexity, when compared to bit loading in conventional OFDM systems. The obtained results show that the effective throughput of P/I-OFDM can be more than fourfold the conventional OFDM while the complexity is less than 1.5%. Moreover, the results show that the peak-to-average power ratio (PAPR) properties of the considered systems are preserved under the adaptation process.

Index Terms—Bit loading, PAPR, OFDM, precoding, adaptive modulation, walsh hadamard.

I. INTRODUCTION

Satisfying quality of service (QoS) is an essential requirement for several emerging applications over wireless networks. Therefore, bit loading, or adaptive modulation, for multicarrier systems such as orthogonal frequency division multiplexing (OFDM) has attracted extensive attention in the literature as reported in [1]–[13], and the references listed therein. In most of the work reported in the literature, the goal is to adapt the modulation order for each subcarrier in order to maximize the throughput, while meeting a prespecified bit error rate (BER) threshold [12]. In such systems, the transmitter and receiver should share the channel state information (CSI) for each subcarrier, and might also need to share the outcome of the bit allocation process. More general bit loading scenarios can be obtained by considering different CSI and QoS targets. For example, the authors in [2] proposed

interference-aware adaptive system for device-to-device (D2D) communications, and thus, the adaptation process requires the knowledge of the interference level, in addition to the CSI. An adaptive algorithm for video communications is proposed in [3], where the goal is to maximize the average peak-signal-to-noise-ratio (PSNR) using cross layer optimization.

Although the bit loading process may provide significant throughput improvement, the overhead that accompanies the optimization process is massive, and hence, various techniques have been proposed to reduce such overhead as described in [13] and the references listed therein. Generally speaking, reducing the overhead comes at the expense of throughput reduction, and hence, there is a trade-off that has to be optimized [11]. In addition to the overhead burden, the computational complexity requirements for discrete bit loading is relatively high, even when efficient algorithms are utilized [11]. The complexity is mostly caused by the searching process that is required for most greedy algorithms used in bit loading techniques [12]. Therefore, achieving the ultimate throughput gain by integrating bit loading in practical systems is difficult because of the substantial overhead requirements that may severely deteriorate the effective throughput of the system, and the complexity, which can be prohibitively high for implementation using most available platforms.

Despite its many advantages, the BER of OFDM is generally similar to single carrier systems in frequency-selective fading channels. Therefore, extensive research has been devoted to improve the BER performance of OFDM. For example, [14] and [15] proposed using linear precoding techniques to introduce frequency diversity, which may significantly improve the BER in frequency-selective channels. Precoded OFDM (POFDM) offers full frequency diversity using Walsh Hadamard transform (WHT) and minimum mean square error (MMSE) equalizer. More recently, the authors of [16] demonstrated that using sub-band POFDM may enhance the immunity of OFDM to narrowband interference. The performance of POFDM over powerline communications with impulse noise is considered in [17] using various equalization techniques. The presented results show that POFDM outperforms the conventional OFDM in such scenarios. An OFDM that utilizes time-domain interleaving (IOFDM) is proposed in [18], where it is shown that time and frequency diversity can be jointly achieved. The IOFDM BER performance is superior in frequency-selective channels with impulse noise.

In this correspondence, we propose an efficient approach to reduce the complexity and overhead of adaptive OFDM systems simultaneously, and hence, the effective throughput and computational complexity are jointly enhanced. Namely, we consider a class of OFDM-based systems where the fading channel coefficients are equal across all subcarriers in each OFDM symbol such as the Walsh Hadamard POFDM [14]–[17], and the IOFDM [18]. Then, a highly efficient bit loading algorithm is designed to operate with very low overhead and complexity. Consequently, it is shown that such systems have an additional key advantage further to the frequency diversity [14]–[18] and peak-to-average power ratio (PAPR) reduction [14]–[17]. The obtained results show that, in certain scenarios, the effective throughput for such systems using the derived bit loading algorithm is more than fourfold the conventional OFDM with a complexity that is less than 1.5%, while preserving other features such as the PAPR reduction.

The rest of the paper is organized as follows. In Section II, the P/I-OFDM system and channel models are presented. Section III introduces the proposed bit loading algorithm for POFDM systems, this section also introduces the complexity and overhead analysis. In Section IV, the numerical results are presented, and finally, Section V concludes the paper.

Manuscript received October 22, 2018; revised February 18, 2019; accepted April 4, 2019. Date of publication April 29, 2019; date of current version July 16, 2019. This work was supported in part by the Center for Cyber Physical systems (C2PS), under Grant RC1-C2PS-T2. The review of this paper was coordinated by Dr. J.-C. Chen. (*Corresponding author: Arafat J Al-Dweik.*)

F. Kalbat and B. Sharif are with the Department of Electrical and Computer Engineering, Khalifa University, 127788 Abu Dhabi, UAE (e-mail: fatma.kalbat@ku.ac.ae; bayan.sharif@ku.ac.ae).

A. Al-Dweik is with the Center for Cyber-Physical Systems (C2PS), Khalifa University, 127788 Abu Dhabi, UAE, and also with the Department of Electrical and Computer Engineering, Western University, London, ON N6A 3K7, Canada (e-mail: dweik@fulbrightmail.org; arafat.dweik@ku.ac.ae).

Y. Iraqi is with the Center for Cyber-Physical Systems (C2PS), Khalifa University, 127788 Abu Dhabi, UAE (e-mail: Youssef.Iraqi@ku.ac.ae).

H. Mukhtar is with the University of Dubai, 14143 Dubai, UAE (e-mail: hhadam@ud.ac.ae).

G. K. Karagiannidis is with the Electrical and Computer Engineering Department, Aristotle University of Thessaloniki, Thessaloniki GR-54124, Greece (e-mail: geokarag@auth.gr).

Digital Object Identifier 10.1109/TVT.2019.2914003

II. P/I-OFDM SYSTEM AND CHANNEL MODELS

A. Precoded OFDM (POFDM)

In POFDM, a sequence of N complex data symbols \mathbf{a} each of which has an average power \mathcal{P}_s is applied to N -point WHT to generate the precoded data sequence $\mathbf{s} = \mathbf{W}\mathbf{a}$, where \mathbf{W} is the normalized N -point Walsh-Hadamard matrix. The composite symbols vector \mathbf{s} is applied to an N -point inverse discrete Fourier transform (IDFT) to generate the time domain samples, similar to conventional OFDM, thus $\mathbf{x} = \mathbf{F}^H \mathbf{s}$, where \mathbf{F}^H is the Hermitian transpose of the discrete Fourier transform (DFT) matrix \mathbf{F} . At the receiver, after discarding the P cyclic prefix (CP samples) and applying the DFT, the sequence \mathbf{r} is produced,

$$\begin{aligned} \mathbf{r} &= \mathbf{H}\mathbf{s} + \boldsymbol{\eta} \\ &= \mathbf{H}\mathbf{W}\mathbf{a} + \boldsymbol{\eta}. \end{aligned} \quad (1)$$

In static fading channels, the channel matrix $\mathbf{H} = \text{diag}\{[H_0, H_1, \dots, H_{N-1}]\}$, $\eta_i \sim \mathcal{CN}(0, \sigma_\eta^2)$, $H_m = \sum_{l=0}^{L_h} h_l e^{-\frac{j2\pi ml}{N}}$ denotes the channel frequency response at subcarrier m , $h_l \sim \mathcal{CN}(0, \sigma_{h_l}^2)$, and $L_h + 1$ is the number of multipath components of the channel.

To extract the data vector \mathbf{a} from (1), the vector \mathbf{r} should be equalized using MMSE equalizer whose output can be expressed as [18]

$$\mathbf{v} = \tilde{\mathbf{H}}\mathbf{H}\mathbf{W}\mathbf{a} + \tilde{\boldsymbol{\eta}} \quad (2)$$

where $\tilde{\boldsymbol{\eta}} = \tilde{\mathbf{H}}\boldsymbol{\eta}$, $\tilde{\mathbf{H}} = \text{diag}\{[\tilde{H}_0, \tilde{H}_1, \dots, \tilde{H}_{N-1}]\}$, and

$$\tilde{H}_m = \frac{H_m^*}{|H_m|^2 + \frac{1}{\Gamma}}. \quad (3)$$

where $(\cdot)^*$ denotes the complex conjugate and $\Gamma \triangleq \mathcal{P}_s/\sigma_\eta^2$ is the average signal-to-noise ratio (SNR). After equalization, the inverse WHT (IWHT) is computed to produce the sequence $\mathbf{d} = \mathbf{W}\mathbf{v}$, where the k th element of \mathbf{d} is given by

$$d_k = \beta_{k,k} a_k + \sum_{n=0, n \neq k}^{N-1} \beta_{k,n} a_n + \zeta_k \quad (4)$$

where $\zeta_k = \sum_{m=0}^{N-1} W_{k,m} \tilde{\eta}_m$ and

$$\beta_{k,n} = \sum_{m=0}^{N-1} W_{k,m} W_{m,n} \tilde{H}_m H_m. \quad (5)$$

The conditional signal-to-interference plus noise ratio (SINR) can be expressed as [14, Eq. 68], [18, Eq. 56]

$$\text{SINR}_{|\mathbf{H}} \triangleq \zeta = \Gamma \frac{\sum_{m=0}^{N-1} \lambda_m}{\sum_{m=0}^{N-1} \frac{\lambda_m}{|H_m|^2}} \quad (6)$$

where $\lambda_m = \tilde{H}_m H_m$. As can be noted from (6), the SINR is independent of the subcarrier index, and hence, all subcarriers will experience the same bit error probability.

B. Time-Domain Interleaved OFDM

In IOFDM [18], the IDFT is interleaved over single or multiple symbols to introduce time and frequency diversity. The results reported in [18] show that when the interleaver dimension is $N \times N$ samples, the SINR of the system will be similar to (6). Therefore, POFDM and IOFDM will have identical BER performance. Due to space limitations, the discussion will focus on POFDM, but the results and conclusions are also applicable to IOFDM.

III. PROPOSED BIT ALLOCATION FOR POFDM

The problem of bit allocation to maximize the throughput under average BER constraints is typically formulated as [12]

$$\max_{b_k} \sum_{k=0}^{N-1} b_k \quad \text{subject to} \quad \frac{\sum_{k=0}^{N-1} b_k P_k}{\sum_{k=0}^{N-1} b_k} \leq P_H \quad (7)$$

where b_i is the number of bits for subcarrier k , P_H is the specified BER threshold, and P_k is the BER for subcarrier k . Once the constraint in (7) is satisfied, the throughput is equal to $\sum_{k=0}^{N-1} b_k$. However, it is more informative to use the normalized throughput, which is the average throughput per subcarrier

$$\Psi \triangleq \frac{1}{N} \sum_{k=0}^{N-1} b_k. \quad (8)$$

The value of $P_k \forall k$ can be computed as described in [11], and its value in conventional OFDM depends on $\gamma_k \triangleq \mathcal{P}_s |H_k|^2 / \sigma_\eta^2$ and the modulation order $M_k^{(n)}$, $n \in \{1, 2, \dots, \varphi\}$, where $M_k^{(1)}$ and $M_k^{(\varphi)}$ represent the lowest and highest possible modulation orders. The set of all possible modulation orders is denoted as \mathbb{M} . The process can be performed in different ways based on where the optimization process is computed, and type of data exchanged between the transmitter and receiver. Nevertheless, it is commonly assumed that $\gamma = [\gamma_0, \gamma_1, \dots, \gamma_{N-1}]$ is initially available only at the receiver who shares it with the transmitter via a feedback channel. The transmitter computes $\mathbf{b} = [b_0, b_1, \dots, b_{N-1}]$, and then shares the result with the receiver.

A. Proposed Bit Allocation

For POFDM, the SNR should be replaced by the SINR ζ (6), which is actually equal for all subcarriers. Consequently, P_k in (7) for a particular channel realization becomes only a function of M because ζ is fixed for all subcarriers, and $P_k = P \forall k$. Similar to conventional OFDM, efficient bit allocation techniques such as the incremental allocation algorithm (IAA) [12] can be used directly to solve (7). However, it is straightforward to show that applying the IAA would result in one of the following three scenarios:

- 1) All subcarriers have the maximum possible modulation order $M_k = M^{(\varphi)} \forall k$.
- 2) All subcarriers have the minimum possible modulation order, $M_k = M^{(1)} \forall k$.
- 3) N_L subcarriers have modulation order $M_k^{(n)}$ and $(N - N_L)$ subcarriers have modulation order $M_k^{(n+1)}$.

For the last case, the constraint in (7) can be written as

$$\frac{N_L m_n P_{|M^{(n)}} + (N - N_L) m_{n+1} P_{|M^{(n+1)}}}{N_L m_n + (N - N_L) m_{n+1}} \leq P_H \quad (9)$$

where $m_x \triangleq \log_2(M^{(x)})$. After some straightforward manipulations, the value of N_L can be computed as

$$N_L = \left\lfloor \frac{N m_{n+1} (P_H - P_{|M^{(n+1)}})}{m_n P_{|M^{(n)}} - m_{n+1} P_{|M^{(n+1)}} - P_H (m_n - m_{n+1})} \right\rfloor \quad (10)$$

where $\lfloor \cdot \rfloor$ denotes the floor function. Therefore, the bit loading process can be implemented efficiently as described in Algorithm 1, where the proposed algorithm is denoted as the direct bit loading algorithm (DBLA). The output of Algorithm 1 is the modulation order index n and the number of subcarriers with modulation order $M^{(n)}$, which can be used to calculate M_k for all subcarriers as,

$$M_k = \begin{cases} M^{(n)}, & k \leq N_L - 1, \varphi > n > 0 \\ M^{(n+1)}, & k > N_L - 1, \varphi > n > 0 \\ 1 & n = 0 \\ M^{(\varphi)} & n = \varphi \end{cases}. \quad (11)$$

Algorithm 1: Direct Bit Loading Algorithm (DBLA).

Input: ζ, P_H, \mathbb{M}
Output: n, N_L

```

1:  for  $n = \varphi : 0$ 
2:      Compute  $P|_{M^{(n)}}$ 
3:      if  $P|_{M^{(n)}} \leq P_H$ 
4:          Break
5:      end if
6:  end for
7:  if  $\varphi > n > 0$ 
8:      Compute  $N_L|_{[M^{(n)}, M^{(n+1)}]}$  using (10)
9:  end if
10: if  $n = 0$  or  $n = \varphi$ 
11:      $N_L = N$ 
12: end if

```

As can be noted from (11), if the BER using the minimum modulation order $M^{(1)}$ does not satisfy the BER constraint, all subcarriers are nulled.

It is worth noting that Algorithm 1 can be applied to IOFDM systems as well because the SINR can be described using (6). However, the number of subcarriers N in (10) is replaced with N^2 because the modulation orders are allocated to N^2 subcarriers as compared to N subcarriers for POFDM.

In mobile fading channels, the bit loading process is affected in two ways, first, the channel matrix \mathbf{H} in (1) becomes non-diagonal, which introduces additional inter-carrier interference (ICI) term to (4). Therefore, the bit loading process in mobile channels should be performed while considering the effect of ICI whose power can be computed as described in [20, Eq. 37]. Nevertheless, for vehicle speed of less than 100 km/h, the ICI power is insignificant and the BER at low and moderate SNRs is mostly determined by the AWGN and fading. Therefore, to avoid estimating the Doppler shift and ICI power, an SNR safety margin can be introduced by considering the worst case scenario. For example, for speeds that are less than 100 km/h, the SNR margin is about 0.1 dB at BER of 10^{-3} [20].

The second effect is that the channel variation increases the CSI exchange rate between the transmitter and receiver, and consequently, it reduces the effective throughput. In several applications that involve mobile channels, it is typically assumed that the channel remains fixed for a time period that is equal to the coherence time of the channel. However, such assumption is not valid for bit loading because the CSI becomes outdated, and hence, the BER constraint could be violated. Consequently, satisfying the BER constraint in mobile channels may require the CSI to be updated for each transmitted symbol.

B. Complexity and Overhead Analysis

The complexity of adaptive bit loading algorithms is usually dominated by the number of times P_k is computed, denoted as C , and hence it is used to indicate the complexity in this work [11]. For the DBLA, Algorithm 1 shows that C is random, and $1 \leq C \leq \varphi - 1$, which is significantly smaller than the IAA used with conventional OFDM where $N \leq C \leq N(\varphi - 1)$. Therefore, the DBLA complexity is about $1/N$ of the IAA.

Adaptive bit loading requires the knowledge of $\gamma_k, k = [0, 1, \dots, N - 1]$, at the transmitter side, which is typically estimated at the receiver, and then sent to the transmitter. On the other hand, the receiver should have $M_k^{(n)} \forall k$. For POFDM systems, the transmitter needs to know only ζ , and the receiver should have N_L and m_n . By noting that $0 < N_L \leq N$ and $m_n \leq \log_2(\varphi)$, then the total overhead is actually negligible as compared to conventional OFDM systems. Moreover, because the complexity is extremely low, it can be implemented at both the transmitter and receiver, and hence, the receiver can directly

compute N_L and m_n . Therefore, the total overhead is limited to ζ , which should be no more than 10 bits for all practical considerations.

Therefore, there are two metrics that can be used, namely, the normalized throughput Ψ defined in (8), which can be used to evaluate the efficiency of the bit loading process, and the effective throughput Ψ_E , which takes the overhead bits into consideration,

$$\Psi_E = \frac{K \sum_{k=0}^{N-1} b_k}{K \sum_{k=0}^{N-1} b_k + \Omega_{RT} + \Omega_{TR}} \quad (12)$$

where K is the number of OFDM symbols transmitted using the same CSI, which is a function of the channel variation rate, Ω_{RT} and Ω_{TR} denote the number of overhead bits sent from the receiver to the transmitter, and vice versa. In mobile channels, the channel parameters change continuously, which implies that the system should use $K = 1$. In high speed applications, it might be even necessary to perform the bit loading using predicted CSI to overcome the impact of the time delay caused by the channel estimation at the receiver side and the propagation time between the receiver and transmitter [21].

IV. NUMERICAL RESULTS

This section presents the performance of the proposed adaptive POFDM (A-POFDM), in terms of throughput, PAPR and complexity. An OFDM system is considered where $N = 128$, and cyclic prefix of $N_{CP} = 32$. The set of modulation schemes used are 64-QAM, 16-QAM, QPSK and BPSK, in addition, subcarriers can be turned off. Two channel models are considered in this work, the Typical Urban (TU) and the Bad Urban (BU) multipath Rayleigh fading [19]. The TU consists of 5 taps with average gains of [0.5682, 0.2388, 0.0951, 0.06, 0.0379], normalized delays of [0, 1, 3, 5, 10] samples and maximum delay spread of 11 samples. The BU consists of 5 taps as well with average gains [0.4584, 0.147, 0.0928, 0.1851, 0.1167], normalized delays [0, 2, 3, 10, 13] and maximum delay spread of 14 samples. The channel coefficients correspond to a quasi-static fading model where the channel remains fixed for K OFDM symbols. Each Monte Carlo simulation run includes 10^5 channel realizations. The proposed algorithm is compared with the adaptive bit loading algorithm proposed by Wyglinski [12] for OFDM systems which is denoted as A-OFDM.

Fig. 1 shows the throughput Ψ versus SNR for various P_H values using A-OFDM and A-POFDM. It is interesting to note that conventional A-OFDM outperforms the A-POFDM for the entire range of SNR and for the three considered thresholds, even though the BER of POFDM is significantly less than OFDM in such channels. Such counterintuitive results are due to the fact that a deep fade over a few subcarriers can be easily mitigated in the A-OFDM by switching off the weakest subcarriers, while it will be spread over all subcarriers in the case of A-POFDM.

Fig. 2 presents the effective throughput Ψ_E , which considers the effect of overhead. For example, using efficient feedback techniques as the one described in [13], then $\Omega_{RT} = 8N_{CP} = 256$ bits given that each channel tap is represented by 8 bits. Moreover, $\Omega_{TR} = \lceil \log_2 \varphi \rceil N = 384$ bits given that $\varphi = 5$. Therefore, the total overhead per channel realization is 640 bits. For the A-POFDM, ζ is represented using 10 bits, which is sufficiently large for such purposes. The numerical results of Fig. 2 show that in fast time-varying channels where $K = 1$, the A-POFDM outperforms the conventional A-OFDM by about 485% at SNR of 5.85 dB, which is the maximum gain that can be achieved for the case of $K = 1$. As Ψ_E starts to saturate at SNR ~ 15 dB, the difference between the two systems starts to decrease where it becomes 83.5% at SNR = 30 dB. For slow time-varying channels, the CSI is updated less frequently, and hence, large values of K can be used. Consequently, the effective throughput of both systems improves as a result of decreasing the overhead. However, the A-OFDM is more sensitive to varying K because of the large overhead required for such systems. By considering $K = 10$, for example, it can be noted that the A-POFDM may outperform the A-OFDM by about 136.3% at SNR = 3.25, which is the maximum difference for this case. At SNR = 30 dB, the difference becomes about 8.5%.

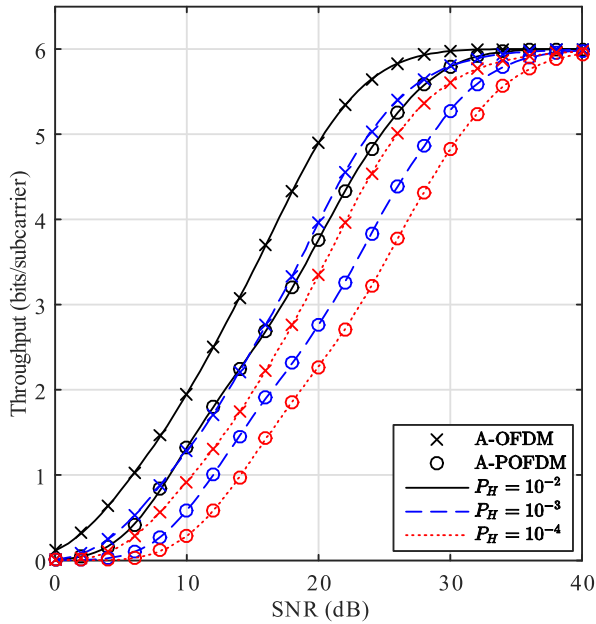


Fig. 1. The throughput Ψ of the A-OFDM and A-POFDM versus SNR for different BER thresholds using the TU channel model.

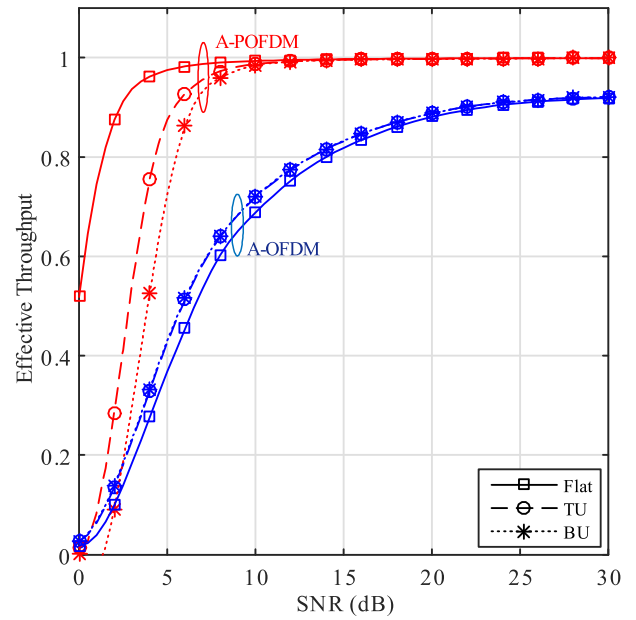


Fig. 3. The effective throughput Ψ_E using different channel models, $K = 10$ and $P_H = 10^{-3}$.

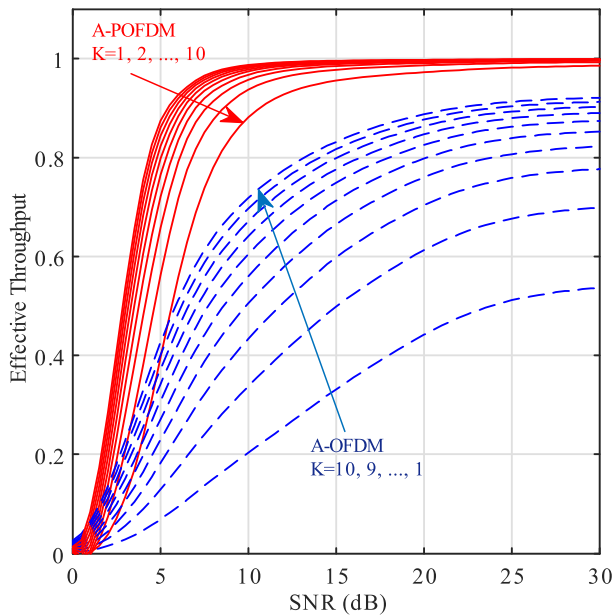


Fig. 2. The effective throughput Ψ_E versus SNR in TU channel for $K = 1, 2, \dots, 10$, and $P_H = 10^{-3}$.

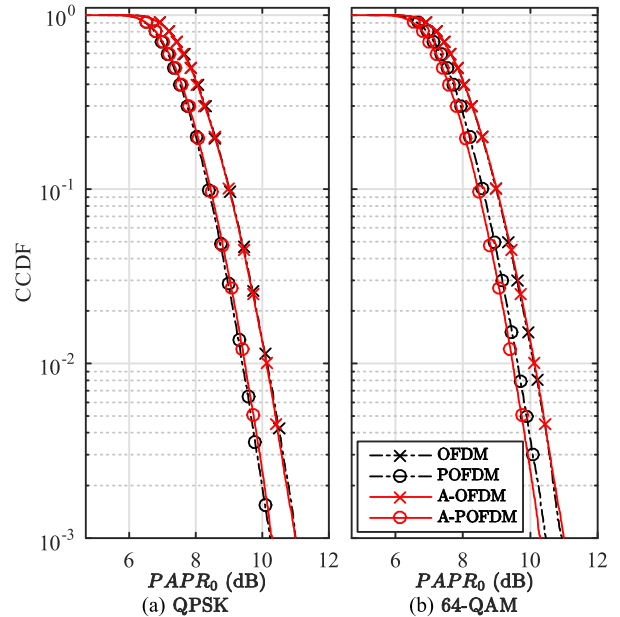


Fig. 4. CCDF for OFDM, A-OFDM, POFDM, and A-POFDM systems.

Fig. 3 shows the effective throughput Ψ_E using three different channels with different frequency selectivity, which are the TU, BU [19], and the flat fading channel. The TU has a normalized root-mean-squared delay spread $\tau_{rms} = 2.22$ samples, and the BU has $\tau_{rms} = 4.91$ samples, and the flat fading has $\tau_{rms} = 0$. As expected, the effective throughput of the A-POFDM is inversely proportional to τ_{rms} , which is due to the fact that deep fades affect all subcarriers within the POFDM symbol. In severely selective channels, it is highly likely that the frequency response of the channel will have multiple nulls, as compared to a single null in the flat fading channel. Therefore, the throughput in the case of frequency-selective channels is expected to be less than the

flat fading channel. In conventional OFDM, the throughput is generally independent of the frequency selectivity of the channel, except for the flat fading case, where a deep fade implies that all subcarriers will be nulled. Therefore, the throughput for the flat fading case is slightly less than the TU and BU channels at low SNRs.

Fig. 4 depicts the complementary cumulative distribution function (CCDF) of the PAPR for the A-OFDM, A-POFDM, conventional OFDM and POFDM signals modulated using QPSK and 64-QAM, an oversampling factor of four [14], $SNR = 20$ dB and $P_H = 10^{-3}$. As can be noted from the figure, the PAPR is generally independent of the modulation order and adaptive bit loading process. Therefore, POFDM and A-POFDM maintain a 0.7 dB advantage over the OFDM and A-OFDM.

TABLE I
AVERAGE NUMBER OF BER OPERATIONS PER OFDM SYMBOL FOR A-POFDM
AND A-OFDM

SNR (dB)	0	10	20	30	40	50
A-POFDM	4	4	3.9	2.2	1.04	1
A-OFDM	512	443	261	141	129	128
C_R %	0.78	0.9	1.5	1.5	0.8	0.78

Although the upper and lower bounds for the computational complexity C of IAA and DBLA are known, the actual value of C is a random function of the SNR and the channel matrix \mathbf{H} . Therefore, Monte Carlo simulation is used to evaluate the complexity more accurately, and the results are presented in Table I for various SNR values. The table also shows the relative complexity C_R , which is the ratio of the $C_{A-POFDM}$ and C_{A-OFDM} . As shown in Table I, the value of C for both systems takes its maximum value at low SNR because the IAA has to search for the solution over all possible states. Nevertheless, the number of states of the IAA is significantly larger than the DBLA where C_R is about 0.78%. On the other extreme of very high SNR, both algorithms converge directly to the optimum solution, which requires the minimum number of iterations, i.e., N for the A-OFDM and 1 for the A-POFDM. Therefore, C_R for this SNR value is similar to the 0 dB case, which is 0.78%. Consequently, the proposed bit loading computational complexity is significantly less than the conventional A-OFDM.

It is also worth comparing the complexity of the proposed algorithm with the results of [4] and [5], although they tackle the bit loading problem from a different perspective. In [4] and [5], the complexity is given in terms of the average number of operations per subcarrier, which is 40 [4, Table II] and 70.76 [5, Table II]. For the proposed algorithm worst case scenario, the BER should be computed φ times regardless of the number of subcarriers, where φ is the number of possible modulation orders. Moreover, φ comparisons are needed while N_L should be computed only once. Therefore, the total number of operations is 15 as compared to $40N$ and $70.76N$ for [4] and [5], respectively.

As can be noted from the obtained throughput results and complexity analysis [14], employing POFDM in frequency-selective channels may offer significant advantages in terms of BER and PAPR reduction. However, POFDM has higher complexity than OFDM due to the additional IWHT and WHT operations at the transmitter and receiver, respectively. Therefore, including the bit loading process in the comparison between OFDM and POFDM reduces the complexity gap between the two schemes and adds a new advantage for POFDM.

V. CONCLUSION

This work proposed a new low-complexity bit loading allocation algorithm for A-POFDM systems in frequency-selective fading channels with BER constraints. The bit loading objective is to maximize the overall throughput while guaranteeing that the BER remains below a prescribed threshold. The algorithm uses the fact that all subcarriers in each POFDM symbol have the same SINR, which significantly reduced the computational complexity and processing time of the optimization process. An interesting and counterintuitive observation is that the throughput of A-OFDM is higher than that of A-POFDM because A-OFDM avoids the deep fading by switching off severely faded subcarriers, which is not possible in A-POFDM. However, the low overhead required by A-POFDM is remarkably small, which makes the effective throughput much higher than the A-OFDM throughput. The analytical and simulation results show that the computational complexity of A-POFDM can be obtained in a few simple steps without the need for exhaustive search, more specifically, the complexity of A-POFDM is less than 1.5% as compared to A-OFDM. The PAPR properties of both A-POFDM and A-OFDM

were generally not affected by the adaptation process, and hence, the A-POFDM has an advantage in this regard as well.

REFERENCES

- [1] F. Halabi, L. Chean, R. P. Giddings, A. Hami, and J. M. Tang, "Multilevel subcarrier index-power modulated optical OFDM with adaptive bit loading for IMDD PON systems," *IEEE Photon. J.*, vol. 8, no. 6, Dec. 2016, Art. no. 7907114.
- [2] S. Sharma, N. Gupta, and V. A. Bohara, "OFDMA-based device-to-device communication frameworks: Testbed deployment and measurement results," *IEEE Access*, vol. 6, pp. 12019–12030, 2018.
- [3] S. Tseng and Y. Chen, "Average PSNR optimized cross layer user grouping and resource allocation for uplink MU-MIMO OFDMA video communications," *IEEE Access*, vol. 6, pp. 50559–50571, 2018.
- [4] T. Vo, K. Amis, T. Chonavel, and P. Siohan, "A low-complexity bit-loading algorithm for OFDM systems under spectral mask constraint," *IEEE Commun. Lett.*, vol. 20, no. 6, pp. 1076–1079, Jun. 2016.
- [5] T. Vo, K. Amis, T. Chonavel, and P. Siohan, "A computationally efficient discrete bit-loading algorithm for OFDM systems subject to spectral-compatibility limits," *IEEE Trans. Commun.*, vol. 63, no. 6, pp. 2261–2272, Jun. 2015.
- [6] D. Wang, Y. Cao, L. Zheng, and Z. Du, "Iterative group-by-group bit-loading algorithms for OFDM systems," *IEEE Trans. Veh. Technol.*, vol. 62, no. 8, pp. 4131–4135, Oct. 2013.
- [7] O. Amin and M. Uysal, "Optimal bit and power loading for amplify-and-forward cooperative OFDM systems," *IEEE Trans. Wireless Commun.*, vol. 10, no. 3, pp. 772–781, Mar. 2011.
- [8] D. Wang, Y. Cao, and L. Zheng, "Efficient two-stage discrete bit-loading algorithms for OFDM systems," *IEEE Trans. Vehic. Technol.*, vol. 59, no. 7, pp. 3407–3416, Sep. 2010.
- [9] H. Elfadil, M. Maleki, and H. Bahrami, "A novel low-complexity adaptive bit mapping scheme for spatial modulation," *IEEE Trans. Vehic. Technol.*, vol. 67, no. 4, pp. 3674–3678, Apr. 2018.
- [10] C. Zhao and K. Kwak, "Power/bit loading in OFDM-based cognitive networks with comprehensive interference considerations: The single-SU case," *IEEE Trans. Vehic. Technol.*, vol. 59, no. 4, pp. 1910–1922, May 2010.
- [11] Y. Iraqi, A. Al-Dweik, and M. Kalil, "Low-complexity slot-based bit loading for multicarrier wireless systems," in *Proc. IEEE 87th Veh. Technol. Conf.*, Porto, Portugal, Jun. 2018, pp. 1–6.
- [12] A. M. Wyglinski, F. Labeau, and P. Kabal, "Bit loading with BER constraint for multicarrier systems," *IEEE Trans. Wireless Commun.*, vol. 4, no. 4, pp. 1383–1387, Jul. 2005.
- [13] N. A. Aly, A. Al-Dweik, and M. Al-Mualla, "Adaptive OFDM system with limited feedback using truncated channel impulse response," in *Proc. IEEE Int. Symp. Signal Process. Inf. Technol.*, Abu Dhabi, UAE, Dec. 2015, pp. 1–6.
- [14] M. Ahmed, S. Boussakta, B. S. Sharif, and C. C. Tsimenidis, "OFDM based on low complexity transform to increase multipath resilience and reduce PAPR," *IEEE Trans. Signal Process.*, vol. 59, no. 12, pp. 5994–6007, Dec. 2011.
- [15] S. Wang, S. Zhu, and G. Zhang, "A Walsh-Hadamard coded spectral efficient full frequency diversity OFDM system," *IEEE Trans. Commun.*, vol. 58, no. 1, pp. 28–34, Jan. 2010.
- [16] O. Popescu and D. C. Popescu, "On the performance of sub-band precoded OFDM in the presence of narrowband co-channel interference," *IEEE Trans. Broadcast.*, vol. 62, no. 3, pp. 736–743, Sep. 2016.
- [17] A. Khan and S. Y. Shin, "Linear precoded wavelet OFDM-based PLC system with overlap FDE for impulse noise mitigation," *Int. J. Commun. Syst.*, vol. 30, no. 17, Nov. 2017, Art. no. e3349.
- [18] M. Mirahmadi, A. Al-Dweik, and A. Shami, "BER reduction of OFDM based broadband communication systems over multipath channels with impulsive noise," *IEEE Trans. Commun.*, vol. 61, no. 11, pp. 4602–4615, Nov. 2013.
- [19] K. Fazel and S. Kaiser, *Multi-Carrier and Spread Spectrum Systems: From OFDM and MC-CDMA to LTE and WiMAX*, Hoboken, NJ, USA: Wiley, 2008.
- [20] A. Al-Dweik, F. Kalbat, S. Muhaidat, O. Filio, and S. M. Ali, "Robust MIMO-OFDM system for frequency-selective mobile wireless channels," *IEEE Trans. Vehic. Technol.*, vol. 64, no. 5, pp. 1739–1749, May 2015.
- [21] A. Khrwat, B. S. Sharif, C. C. Tsimenidis, S. Boussakta, and A. J. Al-Dweik, "Channel prediction for limited feedback precoded MIMO-OFDM systems," in *Proc. IEEE Int. Symp. Signal Process. Inf. Technol. (ISSPIT)*, Dec. 2009, pp. 195–200.